Desalination and Water Treatment
www.deswater.com
doi: 10.1080/19443994.2015.1083889

57 (2016) 17030–17038
August

Taylor & Francis
Taylor & Francis Group

Novel bentonite particle electrodes based on Fenton catalyst and its application in Orange II removal

Nannan Qiao, Jiali Chang, Mengxiao Hu, Hongzhu Ma*

School of Chemistry and Chemical Engineering, Shaanxi Normal University, Xi'An 710119, China, Tel. +86 29 81530726; Fax: +86 29 81530727; emails: qiaonannan.n@snnu.edu.cn (N. Qiao), 1171933088@qq.com (J. Chang), mengxiao0501@snnu.edu.cn (M. Hu), hzmachem@snnu.edu.cn (H. Ma)

Received 29 December 2014; Accepted 11 August 2015

ABSTRACT

Novel particle electrodes, Fe species-modified bentonite (Fe-Bent) were synthesized using a rapid and completely green method employing aqueous green tea extracts as both the reducing and capping agents. The prepared Fe-Bent was characterized using UV–vis spectra, X-ray diffraction, Brunauer–Emmett–Teller, and Fourier transform infrared spectra techniques, and then utilized as heterogeneous Fenton catalyst to constitute a three-dimensional electro-Fenton (3D/E-Fenton) system for decolorization of orange II in aqueous solution. Batch experiment results show that 98.89 and 71.57% of decolorization and chemical oxygen demand (COD) removal were obtained at 0.5 g of Fe-Bent dosage, 0.05 mol L^{-1} Na_2SO_4, and initial solution pH of 6.4, respectively. The evolution of instantaneous current efficiency shows that the 3D/E-Fenton system exhibited higher efficiency for orange II degradation than that of 2D system. In addition, the possible mechanism of the 3D/E-Fenton system in the degradation of orange II was also discussed.

Keywords: Fe-Bent; Green tea extracts; Orange II; 3D/E-Fenton

1. Introduction

In recent years, three-dimensional (3D) electrochemical reactor has received great attention in the field of various wastewater treatments based on its higher current density, higher efficiency, and more extensive interfacial electrode surface areas compared to traditional two-dimensional (2D) system [1,2]. In 3D system, particle electrodes are one of the most important factors [3]. At present, the particle electrodes used mainly including granular activated carbon (GAC) [4], metal particles [5], carbon aerogels [6], and clays [7].

Abundantly found in nature, clay minerals, such as bentonite, are environmentally friendly and much cheaper than others. Meanwhile, the thermal and structural stability of clay minerals make them suitable for hosting metal nanoparticles such as iron-based particles [8], then can be used as a heterogeneous Fenton catalyst and established a three-dimensional electro-Fenton (3D/E-Fenton) system. In the coupled system, H_2O_2 generated continuously on the cathode fed with O_2 (Eq. (1)), that can avoid the cost and danger of transport and storage [9,10]. Then, ·OH produced with the introduction of particle electrodes into the solution (Eq. (2)) [11], derived from Fe^{2+} reacts with H_2O_2, extending the Fenton process (Eqs. (3) and (4)) [5,12]:

*Corresponding author.

$$O_2(g) + 2H^+ + 2e^- \rightarrow H_2O_2 \quad (1)$$

$$Fe^{2+} + H_2O_2 \rightarrow Fe^{3+} + OH^- + {}^{\cdot}OH \quad (2)$$

$$Fe^{3+} + H_2O_2 \leftrightarrow Fe(OOH)^{2+} + H^+ \quad (3)$$

$$Fe(OOH)^{2+} \rightarrow Fe^{2+} + HO_2^{\cdot} \quad (4)$$

So far, several methods have been developed for the synthesis of iron nanoparticles, including sodium borohydride ($NaBH_4$) reduction [13], ethylene glycol reduction and stabilization [14], and carbothermal synthesis [15]. While the toxic chemicals (like $NaBH_4$), organic solvents, or non-biodegradable stabilizing agents, are employed in these methods, which are harmful to the environment [16]. Consequently, a completely green synthesis route of iron-based particles must be developed [17].

Recently, synthesis of iron particles derived from plant polyphenols has attracted much attention [16]. Plant polyphenols extracted from the green materials, such as banana peel, tea, coffee, and eucalyptus could act as both reducing and capping agents [18]. Moreover, polyphenols are biodegradable, nontoxic, and water soluble at room temperature [19]. The iron–polyphenol nanoparticles were prepared with the extracts of *Eucalyptus tereticornis*, *Melaleuca nesophila*, and *Rosmarinus officinalis*, and used for the degradation of acid black 194. The batch experiments showed that 100% decolorization of acid black 194 was obtained, and over 87% total organic carbon (TOC) was removed [20]. Ninety percent bromothymol blue was removed when iron nanoparticles were applied as the Fenton catalyst derived from aqueous sorghum extracts [21]. Ahmmad et al. [22] have synthesized mesoporous α-Fe_2O_3 nanoparticles from the extract of green tea (*Camellia sinensis*) leaves by a green synthesis method, and found that activity was two times higher than commercial α-Fe_2O_3 in terms of ·OH formation. Wang et al. [23] synthesized iron nanoparticles (EL-Fe NPs) through a one-step room-temperature biosynthetic route using eucalyptus leaf extracts, its reactivity in swine wastewater treatment was evaluated and 71.7% of total N and 84.5% of chemical oxygen demand (COD) were removed, respectively. FT-IR spectroscopy showed that some polyphenols were bound to the surfaces of EL-Fe NPs as a capping/stabilizing agent. The iron nanoparticles were found to be nontoxic and highly efficient when compared with the conventional $NaBH_4$ reduction method. Meanwhile, the iron nanoparticles were effectively capped by the tea polyphenols, which can extend their lifetime efficiency [17,21]. However, to our knowledge, iron nanoparticles synthesized from the plant extracts have not been employed as E-Fenton catalysts in 3D electrochemical system to degrade orange II.

Herein, Fe species-modified bentonite (Fe-Bent) was readily synthesized using the liquor of commercially available green tea in the presence of bentonite and used as the particle electrodes in a 3D/E-Fenton system, which was evaluated in degradation of orange II. The objectives included (1) one-pot synthesis of Fe-Bent nanoparticles using green tea extracts; (2) characterizing Fe-Bent with UV–vis, Brunauer–Emmett–Teller (BET), Fourier transform infrared (FT-IR), and X-ray diffraction (XRD); (3) optimizing the parameters, such as pH, Fe-Bent dosage, and electrolyte type on the degradation efficiency of orange II; and (4) evaluating the evolution of instantaneous current efficiency (ICE), Fe leaching behaviors, and possible mechanism of the 3D/E-Fenton system in degradation of orange II.

2. Experimental section

2.1. Materials

The raw bentonite was supplied by Henan, China. Analytical grade $Fe(NO_3)_3{\cdot}9H_2O$, Na_2SO_4, and orange II were purchased from Sinopharm Chemical Reagent Co. Ltd. Green tea was collected from Zhejiang, China. The chemical structure of orange II was depicted in Fig. 1.

2.2. Preparation of Fe-Bent nanoparticles

Tea extract preparation: The tea extract was prepared by heating 37.5 g L^{-1} green tea until boiling. After settling for 1.0 h, the extract was vacuum filtered and stored at room temperature for further use.

Fe-Bent nanoparticles preparation: 0.1 mol L^{-1} Fe $(NO_3)_3$ solution was added to the freshly filtered tea extracts with a volume ratio of 1:2 with vigorously stirring, the solution turned black immediately (Fe-Tea). Typically, the raw bentonite (2.52 g) was

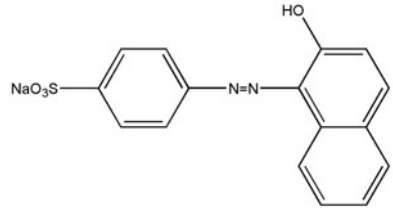

Fig. 1. The molecule structure of orange II.

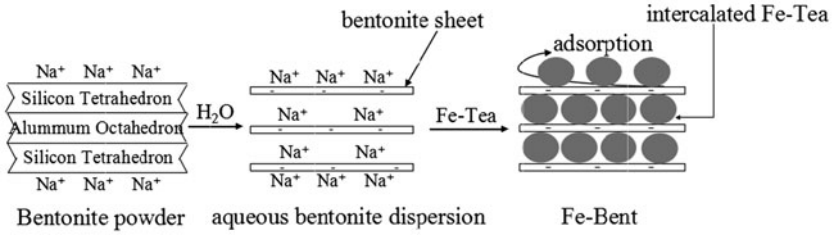

Fig. 2. Synthesis of the Fe-Bent nanoparticles.

dispersed into 150 ml of water in a beaker to form the swollen layers. Then, Fe-Tea was poured into the beaker with vigorously stirring for 4 h. The precipitate was washed with distilled water and ethanol for several times, dried at 60℃ in vacuum for 12 h, and pulverized into powder to obtain Fe-Bent nanoparticles, as illustrated in Fig. 2.

2.3. Batch experiments

The degradation of orange II with Fe-Bent nanoparticles was conducted in an undivided 1-L cylindrical glass reactor (Fig. 3), into which 400 ml of an aqueous solution containing 100 mg L^{-1} of orange II was introduced. Both anode and cathode electrodes were graphite plates with 3.5×6 cm^2 in size and situated 1 cm from each other, and supplied with a constant current density of 14.29 mA cm^{-2}. Fe-Bent nanoparticles were packed between the anode and cathode with air sparged onto the cathode to construct a 3D electrochemical reactor. During the electrolysis process, H_2O_2 was produced *in situ* via oxygen reduction. Samples were taken from the reactor at given time interval and then filtered before further analysis.

2.4. Characterization of Fe-Bent nanoparticles and effluent analysis

The crystallinity of Fe-Bent nanoparticles were detected using an XRD with Cu Kα radiation (D/Max2550VB+/PC, $\lambda = 1.5406$ Å) at 40 kV/100 mA. Diffraction patterns were recorded in the range of 3–60° (2θ) with a scanning rate of 8°/min. The BET specific surface areas were determined with a Micrometerics ASAP 2020 M apparatus (McKesson Corporation, America) by nitrogen adsorption at 77 K. FTIR spectra were recorded on an FT-IR spectrometer (Tensor 27, Bruker, Germany).

The concentrations of leaching iron ions in solution were determined spectrophotometrically (λ at 510 nm) by 1,10-phenanthroline method [24].

The concentration of orange II in the effluent was determined by UV–vis spectrophotometry (UVT6, Beijing Purkinje General Instrument Co. Ltd, China) and the COD values were measured by COD analyzer (5B-3(C), Lanzhou, China). Color removal (R%), COD removal (R_{COD}%), and ICE [25] were calculated by Eqs. (5)–(7):

$$R\% = \frac{A_0 - A_t}{A_0} \times 100\% \tag{5}$$

where A_0 and A_t are the absorbance of the initial and at reaction time t (min), respectively.

$$R_{COD}\% = \frac{COD_0 - COD_t}{COD_0} \times 100\% \tag{6}$$

where COD_0 and COD_t are the COD value (in $gO_2\ dm^{-3}$) at reaction time 0 (min) and t (min), respectively.

$$ICE = \frac{COD_t - COD_{t+\Delta t}}{8I\Delta t} FV \tag{7}$$

where COD_t and $COD_{t+\Delta t}$ are the COD value at time t and $t + \Delta t$ (in $gO_2\ dm^{-3}$), respectively, I is the current

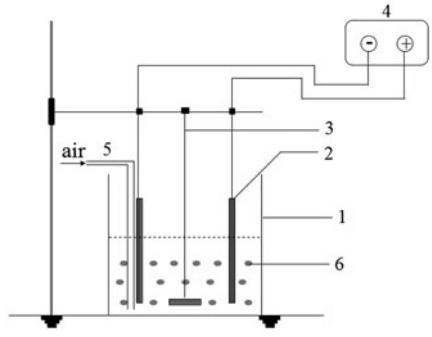

Fig. 3. Sketch of the electrochemical cell.
Notes: (1) Glass reactor, (2) graphite plates, (3) electric stirrer, (4) D.C. power, (5) gas tube and (6) Fe-bent.

(A), F is the Faraday constant (96,487 C mol^{-1}), and V is the volume of solution (dm^3).

3. Results and discussion

3.1. Characterization of Fe-Bent nanoparticles

The formation of Fe species from tea extract (Fe-Tea) was studied using UV spectra (Fig. 4). The reaction between $Fe(NO_3)_3$ and tea extract was instantaneous and the color of the mixture changed from yellow to black promptly (Fig. 4 inset). Moreover, UV spectra of Fe-Tea show that a broad band at higher wavelength appeared, also indicating the formation of Fe-Tea.

FT-IR spectra (Fig. 5) show that the bands at 3,640 and 3,430 cm^{-1} were corresponded to the O–H vibration for Bent and Fe-Bent, respectively [20]. The bands at 1,090 and 1,040 cm^{-1} attributed to Si–O stretching vibration [16]. In addition, the band at 1,640 cm^{-1} for Fe-Bent maybe related to the C=C ring stretching in polyphenols, indicating the formation of the iron–polyphenols complex [20].

The XRD patterns of Bent and Fe-Bent (Fig. 6) show that the basal spacing of Bent ($d_{0\,0\,1}$) shifted from 1.25 nm ($2\theta = 7.06^\circ$) to 1.61 nm ($2\theta = 5.5^\circ$), confirming the intercalation of Fe in the interlayer spaces of the Bent [26]. Compared to reflections of Bent, the XRD peak of Fe-Bent at $2\theta = 10.02^\circ$ totally disappeared, the reflections at $2\theta = 35.00^\circ$–36.25° had a few subtle changes, and the reflections intensity at $2\theta = 27.06^\circ$ and 29.13° was obviously reduced. All these results indicated that the synthesized Fe-Bent nanoparticles were mainly iron oxide on the bentonite [27–29]. However, no obvious reflection of Fe^0 ($2\theta = 44.90^\circ$) was detected in Fe-Bent, suggesting that Fe-Bent nanoparticles were amorphous in nature [30,31]. Moreover, a less obvious characteristic reflection of Fe-Bent was observed at $2\theta = 17.24^\circ$, identified as organic materials adsorbed from tea extract as a capping agent [21], which was consistent with the results of FT-IR (Fig. 5).

The BET specific surface area (S_{BET}), average pore size (d_p), and pore volume (V_p) of Bent and Fe-Bent are shown in Table 1. The S_{BET} and d_p were both decreased dramatically, and V_p decreased slightly from 0.071216 to 0.065473 $cm^3\,g^{-1}$, indicating the

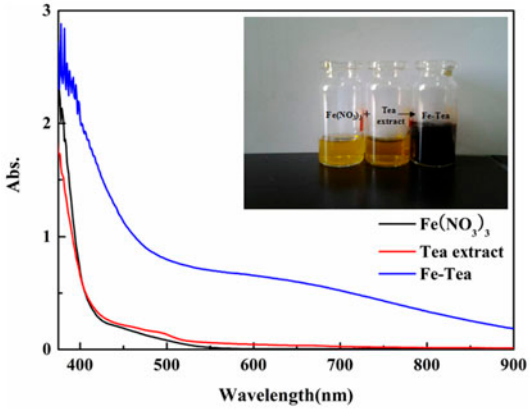

Fig. 4. UV spectra of reactants and Fe-Tea.

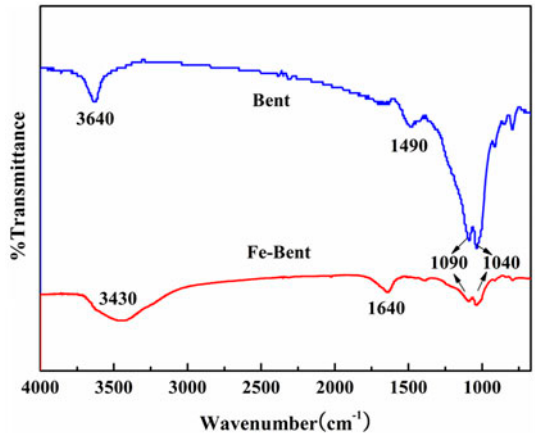

Fig. 5. FT-IR spectra of Bent and Fe-Bent.

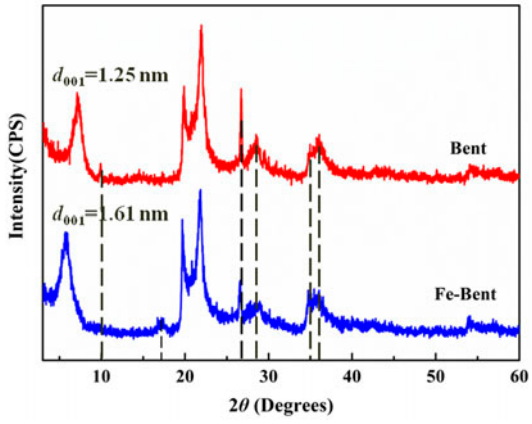

Fig. 6. XRD patterns of Bent and Fe-Bent.

Table 1
Structure properties of Bent and Fe-Bent

Samples	S_{BET} ($m^2\,g^{-1}$)	d_p (nm)	V_p ($cm^3\,g^{-1}$)
Bent	35.1782	63.724	0.071216
Fe-Bent	8.6384	9.2453	0.065473

intercalation of Fe-Tea greatly altered the surface structure distribution of bentonite [32].

3.2. Effects of 3D/E-Fenton system on degradation efficiency of orange II

3.2.1. Effect of initial pH

The pH values play an important role in the azo dye degradation [33]. Therefore, the effect of the initial pH value on the removal of orange II was investigated (Fig. 7), and the optimal catalytic activity exhibited at pH 3. It may be due to the ionization of SO_3^- group was increased and the positive charge of orange II molecules were decreased with pH increasing. However, it should be noted that even at pH 7, 97.86% decolorization still achieved in 60 min, indicating that the Fe-Bent nanoparticles could be used in a wide pH range.

In addition, the adsorption and 3D/E-Fenton process were also compared. The adsorption accounted for 60–70% color removal at the neutral and acidic conditions, indicating that Fe-Bent not only acted as a heterogeneous Fenton catalyst in the electrochemical reactor, but also acted as an effective adsorbent in the whole procedure.

The pH evolution shows that the final pH (60 min) increased slightly when the initial pHs were at 2.01 and 3.02, while decreased for the others. The possible reason was that some acidic intermediates, such as HNO_3 and $NaHSO_4$, were formed (Eq. (8)) during the degradation of orange II [34], which can cause pH decreasing while it was moderate at the very beginning. While the concentrations of HNO_3 and $NaHSO_4$ were relatively lower in more acidic (2–3) solution than that in the moderate condition, hence, no significant change of the solution pH was observed [35].

$$C_{16}H_{11}N_2NaO_4S + {}^{\cdot}OH \rightarrow CO_2 + H_2O + HNO_3 + NaHSO_4 \quad (8)$$

3.2.2. Effect of Fe-Bent dosage

The effect of Fe-Bent dosage on orange II removal is presented in Fig. 8. In the absence of Fe-Bent (0 g), the removal of orange II was lower than 55.04% in 60 min. When 0.5 g Fe-Bent was introduced, the color removal after 60 min increased drastically to 98.89% (3D/E-Fenton system), while 65.84% removal was contributed to the adsorption effect, which was mainly due to the increase in the number of active sites as well as the generation of more hydroxyl radicals [36]. When the Fe-Bent dosage reached 0.75 g, the removal of orange II was declined slightly, that may be due to the agglomeration of Fe-Bent and the side reaction of hydroxyl radicals (Eq. (9)) [37].

$$Fe^{2+} + {}^{\cdot}OH \rightarrow Fe^{3+} + OH^- \quad (9)$$

3.2.3. Effect of electrolyte type

The effect of electrolyte type (Na_2SO_4, NaCl) on the degradation of orange II (Fig. 9) shows that the removal efficiency decreased following the order of $SO_4^{2-} > Cl^-$. This may be assigned to the higher conductivity of SO_4^{2-} than Cl^- [38]. Another possible reason was that hydroxyl radicals were scavenged by Cl^- and $[CLOH]^{\cdot -}$ (Eqs. 10 and 11) [39].

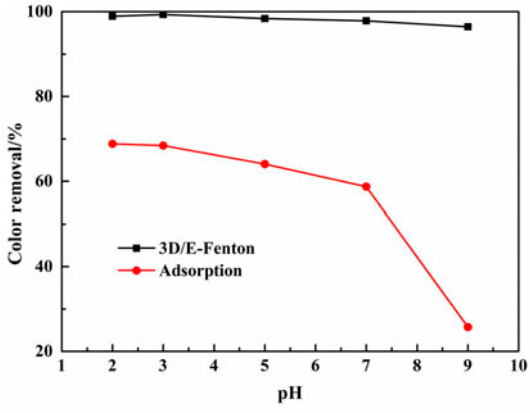

Fig. 7. Effect of pH on orange II removal.

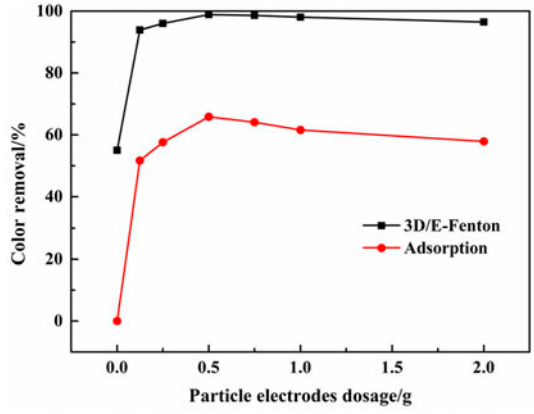

Fig. 8. Effect of Fe-Bent dosage on orange II removal.

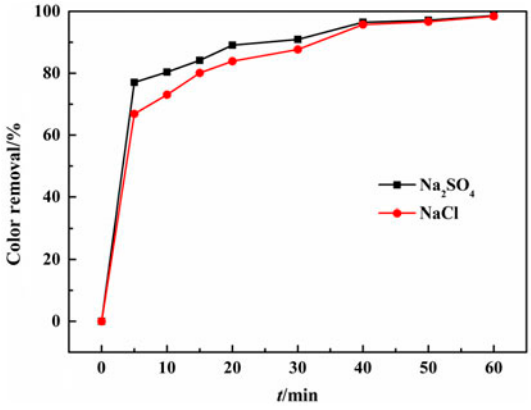

Fig. 9. Effect of electrolyte type on orange II removal.

$$Cl^- + {}^{\cdot}OH \rightarrow [ClOH]^{\cdot -} \quad (10)$$

$$[ClOH]^{\cdot -} + Cl^- \rightarrow Cl_2^{\cdot -} + OH^- \quad (11)$$

3.2.4. Effect of Na_2SO_4 concentration

The orange II removal increased with the increasing concentration of Na_2SO_4 (Fig. 10), in both adsorption and 3D/E-Fenton system. On one hand, higher Na_2SO_4 concentration led to higher current density, which brought about faster and more producing of hydrogen peroxide [40]. On the other hand, the presence of the inorganic and salting-out salt in aqueous solution enhanced the adsorption of orange II onto Fe-Bent [41]. However, when the Na_2SO_4 concentration increased to 0.1 M, the removal of orange II significantly decreased. This may be due to the consumption of the generated hydroxyl radical by SO_4^{2-} as Eq. (12) [39].

$${}^{\cdot}OH + SO_4^{2-} \rightarrow OH^- + SO_4^{\cdot -} \quad (12)$$

3.3. Evolution of ICE with time

The ICE increased sharply at the first 10 min and then decreased (Fig. 11), which attributed to the mass transport limitation and the side reaction of oxygen evolution [1]. The ICE in 3D/E-Fenton system was higher than that in 2D system, suggesting that more oxidants were formed in 3D/E-Fenton system and higher COD removal efficiency was obtained [42]. The significant ICE improvement revealed that 3D/E-Fenton system exhibited higher efficiency than 2D system in azo dye wastewater treatment.

3.4. Recycling of the Fe-Bent

The removal of orange II maintained at 94.27–98.89% in 5 recycles (Fig. 12), with only a slightly decrease, implied that the Fe-Bent displayed much higher stability and reusability during the removal of orange II. There are two possible reasons for the slight decline of the removal of orange II: with the reaction proceeded, ferric oxide and hydroxide formed on the particle electrodes surface, which blocked its reactive sites [8]. On the other hand, a fraction of iron leached from the Fe-Bent, also leading to the decrease in its catalytic activity. Fig. 13 depicts the change of iron ion concentration with the reaction time. The leaching of iron ions decreased with the reaction proceeding indicated that the iron ions in the solution maybe deposited back to the Fe-Bent surface. At the end of

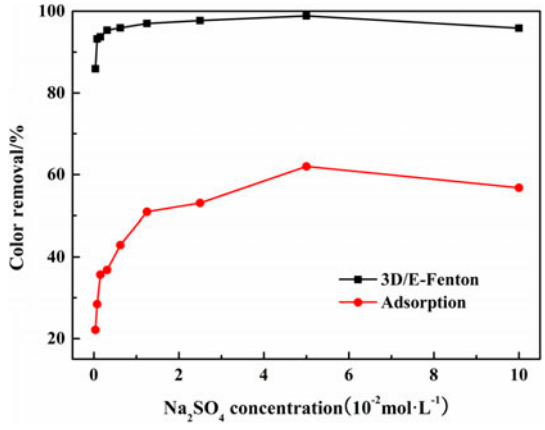

Fig. 10. Effect of Na_2SO_4 concentration on orange II removal.

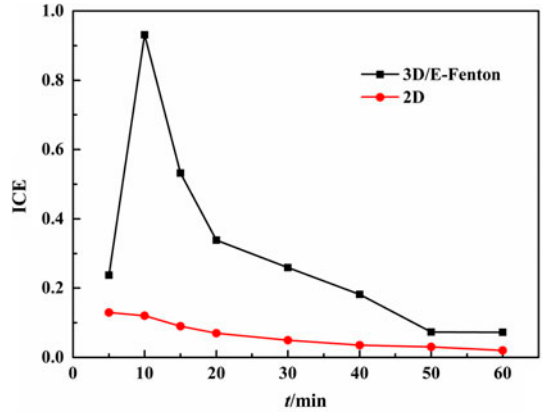

Fig. 11. Evolution of ICE with time.

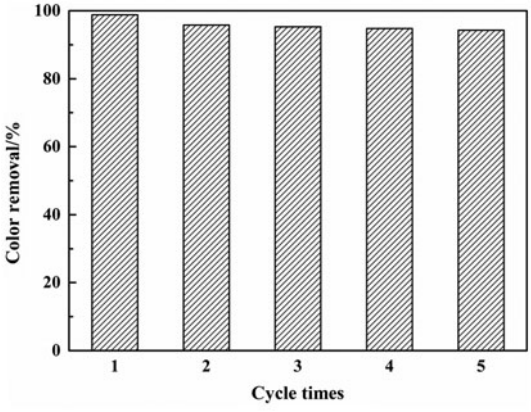

Fig. 12. Recycles of Fe-Bent.

the reaction (60 min), iron leaching was less than 3.84 mg L^{-1}, such a low degree of leaching suggested the stability and reusability of the Fe-Bent particle electrodes, which was consistent with the FT-IR analysis.

3.5. The evolution of orange II removal and solution pH

The evolution of orange II removal and solution pH (Fig. 14) showed that the color removal and COD removal were 98.89 and 71.57% after 60 min, respectively, the solution pH decreased to 5.57, indicating that orange II can be degraded effectively and mineralized incompletely in this 3D/E-Fenton system.

3.6. Possible degradation process of orange II

To clarify the changes of structural characteristics of orange II during the 3D/E-Fenton process, UV–vis spectra were recorded (Fig. 15). A visible band at 486 nm, attributed to azo bonds, was observed at the very beginning [34]. And two peaks in the UV region,

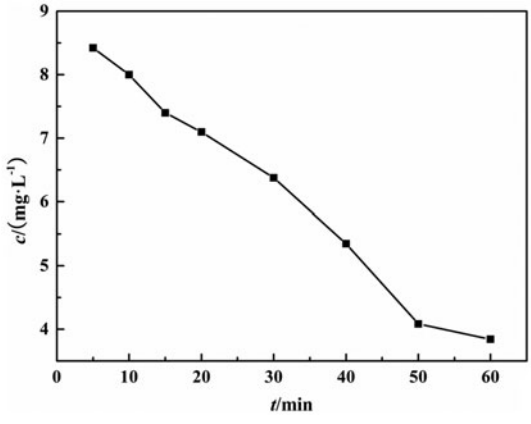

Fig. 13. The leaching of iron ions.

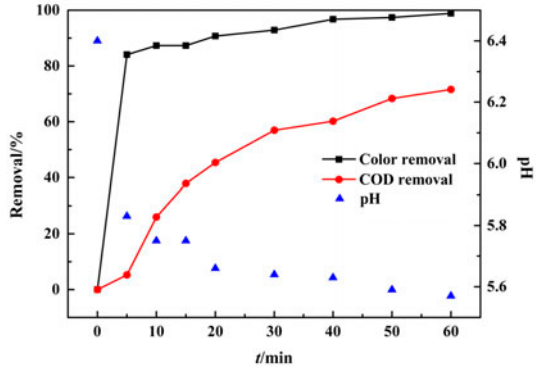

Fig. 14. The evolution of orange II removal and pH under the optimum conditions.

309 and 229 nm, corresponding to π–π* transitions in the naphthalene and benzoic rings of orange II, respectively, were also observed [34]. With the reaction proceeding, the visible band remarkably disappeared, mainly due to the fragmentation of the azo bond by oxidation [43]. However, the appearance of peaks at 206 and 248 nm indicated that the azo dye was not completely mineralized.

3.7. Possible mechanism of 3D/E-Fenton system

Based on the above discussions and the references reported [27,36,44,45], a possible mechanism for 3D/E-Fenton system degradation of orange II was proposed (Fig. 16). Firstly, the Fe-Bent particles acted as adsorbent to adsorb the substrate orange II. Secondly, H_2O_2*in situ* was formed from abundance of active O_2 capturing two electrons on the surface of cathode and diffused into the water bulk phase (Eq. (1)). Meanwhile, once H_2O_2 molecules were generated, it would be decomposed catalytically

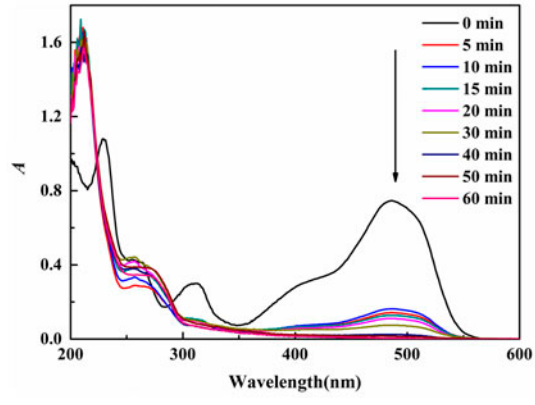

Fig. 15. UV–vis spectra changes as a function of reaction time.

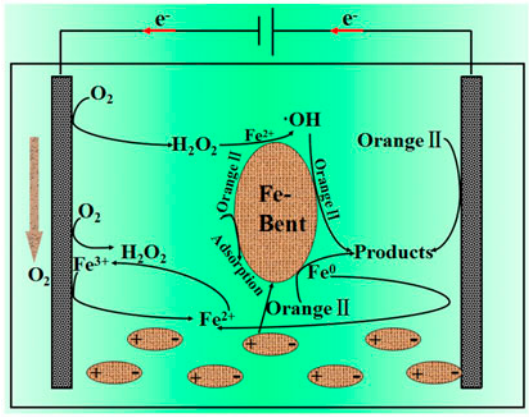

Fig. 16. Possible mechanism of 3D/E-Fenton reactor.

to strong oxidizer ·OH radical by Fe^{2+} (Eq. (2)). Then orange II was degraded by the formed ·OH radical [44].

4. Conclusion

Fe-Bent was prepared one pot from green tea extract and bentonite at room temperature, and employed as an E-Fenton catalyst and the particle electrodes in electrochemical degradation of orange II. With the initial orange II concentration of 100 mg L^{-1}, Fe-Bent dosage of 0.5 g, and Na_2SO_4 concentration of 0.05 mol L^{-1}, 98.89% color removal and 71.57% COD removal were obtained after 60 min. The evolution of ICE indicated that 3D/E-Fenton reactor was more effective than the traditional 2D system. The iron leaching decreased after the reaction, indicating that iron ion deposit back to the Fe-Bent surface, and avoiding the secondary pollution of water quality. It was therefore demonstrated that Fe-Bent was a potential material for the remediation of the azo dye wastewater.

Acknowledgments

The authors are grateful to be supported by the Fundamental Research Funds for the Central Universities (GK201302013).

References

[1] L.Y. Wei, S.H. Guo, G.X. Yan, C.M. Chen, X.Y. Jiang, Electrochemical pretreatment of heavy oil refinery wastewater using a three-dimensional electrode reactor, Electrochim. Acta 55 (2010) 8615–8620.
[2] Z.G. Liu, F.F. Wang, Y.S. Li, T.L. Xu, S.M. Zhu, Continuous electrochemical oxidation of methyl orange waste water using a three-dimensional electrode reactor, J. Environ. Sci. 23 (Supplement) (2011) S70–S73.
[3] Z.Y. Wang, J.Y. Qi, Y. Feng, K. Li, X. Li, Preparation of catalytic particle electrodes from steel slag and its performance in a three-dimensional electrochemical oxidation system, J. Ind. Eng. Chem. 20 (2014) 3672–3677.
[4] L.N. Xu, H.Z. Zhao, S.Y. Shi, G.Z. Zhang, J.R. Ni, Electrolytic treatment of C.I. Acid Orange 7 in aqueous solution using a three-dimensional electrode reactor, Dyes Pigm. 77 (2008) 158–164.
[5] W. Liu, Z.H. Ai, L.Z. Zhang, Design of a neutral three-dimensional electro-Fenton system with foam nickel as particle electrodes for wastewater treatment, J. Hazard. Mater. 243 (2012) 257–264.
[6] X. Wu, X. Yang, D. Wu, R. Fu, Feasibility study of using carbon aerogel as particle electrodes for decoloration of RBRX dye solution in a three-dimensional electrode reactor, Chem. Eng. J. 138 (2008) 47–54.
[7] M.M. Cheng, W.J. Song, W.H. Ma, C.C. Chen, J.C. Zhao, J. Lin, H.Y. Zhu, Catalytic activity of iron species in layered clays for photodegradation of organic dyes under visible irradiation, Appl. Catal., B Environ. 77 (2008) 355–363.
[8] Y.M. Li, J.F. Li, Y.L. Zhang, Mechanism insights into enhanced Cr(VI) removal using nanoscale zerovalent iron supported on the pillared bentonite by macroscopic and spectroscopic studies, J. Hazard. Mater. 227–228 (2012) 211–218.
[9] S. Mohajeri, H.A. Aziz, M.H. Isa, M.A. Zahed, M.N. Adlan, Statistical optimization of process parameters for landfill leachate treatment using electro-Fenton technique, J. Hazard. Mater. 176 (2010) 749–758.
[10] E. Brillas, I. Sirés, M.A. Oturan, Electro-Fenton process and related electrochemical technologies based on Fenton's reaction chemistry, Chem. Rev. 109 (2009) 6570–6631.
[11] X.F. Xu, P. Liao, S.H. Yuan, M. Tong, M.S. Luo, W.J. Xie, Cu-catalytic generation of reactive oxidizing species from H_2 and O_2 produced by water electrolysis for electro-Fenton degradation of organic contaminants, Chem. Eng. J. 233 (2013) 117–123.
[12] F. Martínez, G. Calleja, J.A. Melero, R. Molina, Iron species incorporated over different silica supports for the heterogeneous photo-Fenton oxidation of phenol, Appl. Catal., B Environ. 70 (2007) 452–460.
[13] C.B. Wang, W.X. Zhang, Synthesizing nanoscale iron particles for rapid and complete dechlorination of TCE and PCBs, Environ. Sci. Technol. 31 (1997) 2154–2156.
[14] T. Arun, K. Prakash, R. Justin Joseyphus, Synthesis and magnetic properties of prussian blue modified Fe nanoparticles, J. Magn. Magn. Mater. 345 (2013) 100–105.
[15] M. Razavi, A.H. Rajabi-Zamani, M.R. Rahimipour, R. Kaboli, M.O. Shabani, R. Yazdani-Rad, Synthesis of Fe-TiC-Al_2O_3 hybrid nanocomposite via carbothermal reduction enhanced by mechanical activation, Ceram. Int. 37 (2011) 443–449.
[16] P.K. Tandon, R.C. Shukla, S.B. Singh, Removal of Arsenic(III) from water with clay-supported zerovalent iron nanoparticles synthesized with the help of tea liquor, Ind. Eng. Chem. Res. 52 (2013) 10052–10058.
[17] M.N. Nadagouda, A.B. Castle, R.C. Murdock, S.M. Hussain, R.S. Varma, *In vitro* biocompatibility of nanoscale zerovalent iron particles (NZVI) synthesized using tea polyphenols, Green Chem. 12 (2010) 114–122.

[18] S. Machado, S.L. Pinto, J.P. Grosso, H.P.A. Nouws, J.T. Albergaria, C. Delerue-Matos, Green production of zero-valent iron nanoparticles using tree leaf extracts, Sci. Total Environ. 445–446 (2013) 1–8.
[19] Z.Q. Wang, Iron complex nanoparticles synthesized by eucalyptus leaves, ACS Sustainable Chem. Eng. 1 (2013) 1551–1554.
[20] Z.Q. Wang, C. Fang, M. Megharaj, Characterization of iron–polyphenol nanoparticles synthesized by three plant extracts and their Fenton oxidation of azo dye, ACS Sustainable Chem. Eng. 2 (2014) 1022–1025.
[21] E.C. Njagi, H. Huang, L. Stafford, H. Genuino, H.M. Galindo, J.B. Collins, G.E. Hoag, S.L. Suib, Biosynthesis of iron and silver nanoparticles at room temperature using aqueous sorghum bran extracts, Langmuir 27 (2011) 264–271.
[22] B. Ahmmad, K. Leonard, M.S. Islam, J. Kurawaki, M. Muruganandham, T. Ohkubo, Y. Kuroda, Green synthesis of mesoporous hematite (α-Fe_2O_3) nanoparticles and their photocatalytic activity, Adv. Powder Technol. 24 (2013) 160–167.
[23] T. Wang, X.Y. Jin, Z.L. Chen, M. Megharaj, R. Naidu, Green synthesis of Fe nanoparticles using eucalyptus leaf extracts for treatment of eutrophic wastewater, Sci. Total Environ. 466–467 (2014) 210–213.
[24] L.Q. Guo, F. Chen, X.Q. Fan, W.D. Cai, J.L. Zhang, S-doped α-Fe_2O_3 as a highly active heterogeneous Fenton-like catalyst towards the degradation of acid orange 7 and phenol, Appl. Catal., B Environ. 96 (2010) 162–168.
[25] M. Panizza, C. Bocca, G. Cerisola, Electrochemical treatment of wastewater containing polyaromatic organic pollutants, Water Res. 34 (2000) 2601–2605.
[26] S. Luo, P.F. Qin, J.H. Shao, L. Peng, Q.R. Zeng, J.D. Gu, Synthesis of reactive nanoscale zero valent iron using rectorite supports and its application for Orange II removal, Chem. Eng. J. 223 (2013) 1–7.
[27] Y.M. Lin, Z.X. Chen, Z.L. Chen, M. Megharaj, R. Naidu, Decoloration of acid violet red B by bentonite-supported nanoscale zero-valent iron: Reactivity, characterization, kinetics and reaction pathway, Appl. Clay Sci. 93–94 (2014) 56–61.
[28] T. Shahwan, S. Abu Sirriah, M. Nairat, E. Boyacı, A.E. Eroglu, T.B. Scott, K.R. Hallam, Green synthesis of iron nanoparticles and their application as a Fenton-like catalyst for the degradation of aqueous cationic and anionic dyes, Chem. Eng. J. 172 (2011) 258–266.
[29] Z.H. Pang, M.Y. Yan, X.S. Jia, Z.X. Wang, J.Y. Chen, Debromination of decabromodiphenyl ether by organo-montmorillonite-supported nanoscale zero-valent iron: Preparation, characterization and influence factors, J. Environ. Sci. 26 (2014) 483–491.
[30] Y. Kuang, Q.P. Wang, Z.L. Chen, M. Megharaj, R. Naidu, Heterogeneous Fenton-like oxidation of monochlorobenzene using green synthesis of iron nanoparticles, J. Colloid Interface Sci. 410 (2013) 67–73.
[31] T. Wang, J.J. Lin, Z.L. Chen, M. Megharaj, R. Naidu, Green synthesized iron nanoparticles by green tea and eucalyptus leaves extracts used for removal of nitrate in aqueous solution, J. Cleaner Prod. 83 (2014) 413–419.
[32] J.B. Zhong, J.Z. Li, Z.H. Xiao, W. Hu, X.B. Zhou, X.W. Zheng, Improved photocatalytic performance of ZnO prepared by sol-gel method with the assistance of CTAB, Mater. Lett. 91 (2013) 301–303.
[33] B.H. Moon, Y.B. Park, K.H. Park, Fenton oxidation of Orange II by pre-reduction using nanoscale zero-valent iron, Desalination 268 (2011) 249–252.
[34] J.Y. Feng, X.J. Hu, P.L. Yue, Degradation of azo-dye Orange II by a photoassisted Fenton reaction using a novel composite of iron oxide and silicate nanoparticles as a catalyst, Ind. Eng. Chem. Res. 42 (2003) 2058–2066.
[35] J.Y. Feng, X.J. Hu, P.L. Yue, Effect of initial solution pH on the degradation of Orange II using clay-based Fe nanocomposites as heterogeneous photo-Fenton catalyst, Water Res. 40 (2006) 641–646.
[36] Z.X. Chen, X.Y. Jin, Z.L. Chen, M. Megharaj, R. Naidu, Removal of methyl orange from aqueous solution using bentonite-supported nanoscale zero-valent iron, J. Colloid Interface Sci. 363 (2011) 601–607.
[37] A. Babuponnusami, K. Muthukumar, Treatment of phenol-containing wastewater by photoelectro-Fenton method using supported nanoscale zero-valent iron, Environ. Sci. Pollut. Res. 20 (2013) 1596–1605.
[38] M.M. Ghoneim, H.S.E. Desoky, N.M. Zidan, Electro-Fenton oxidation of Sunset Yellow FCF azo-dye in aqueous solutions, Desalination 274 (2011) 22–30.
[39] N. Daneshvar, S. Aber, V. Vatanpour, M.H. Rasoulifard, Electro-Fenton treatment of dye solution containing Orange II: Influence of operational parameters, J. Electroanal. Chem. 615 (2008) 165–174.
[40] M.H. Zhou, Q.H. Yu, L.C. Lei, G. Barton, Electro-Fenton method for the removal of methyl red in an efficient electrochemical system, Sep. Purif. Technol. 57 (2007) 380–387.
[41] C.M.S.S. Neves, J. Lemus, M.G. Freire, J. Palomar, J.A.P. Coutinho, Enhancing the adsorption of ionic liquids onto activated carbon by the addition of inorganic salts, Chem. Eng. J. 252 (2014) 305–310.
[42] L. Yan, H.Z. Ma, B. Wang, Y.F. Wang, Y.S. Chen, Electrochemical treatment of petroleum refinery wastewater with three-dimensional multi-phase electrode, Desalination 276 (2011) 397–402.
[43] J.H. Ramirez, C.A. Costa, L.M. Madeira, G. Mata, M.A. Vicente, M.L. Rojas-Cervantes, A.J. López-Peinado, R.M. Martín-Aranda, Fenton-like oxidation of Orange II solutions using heterogeneous catalysts based on saponite clay, Appl. Catal., B Environ. 71 (2007) 44–56.
[44] H. Liu, G. Li, J. Qu, H. Liu, Degradation of azo dye Acid Orange 7 in water by Fe^0/granular activated carbon system in the presence of ultrasound, J. Hazard. Mater. 144 (2007) 180–186.
[45] J.A. Mielczarski, G.M. Atenas, E. Mielczarski, Role of iron surface oxidation layers in decomposition of azo-dye water pollutants in weak acidic solutions, Appl. Catal., B Environ. 56 (2005) 289–303.